Ecosystems
https://doi.org/10.1007/s10021-023-00863-z

ORIGINAL ARTICLE

Sustained Three-Year Declines in Forest Soil Respiration are Proportional to Disturbance Severity

Kayla C. Mathes,[1]* Stephanie Pennington,[2] Carly Rodriguez,[3] Ben Bond-Lamberty,[2] Jeff W. Atkins,[1,4] Christoph S. Vogel,[5] and Christopher M. Gough[1]

[1]*Department of Biology, Virginia Commonwealth University, 1000 West Cary St., Box 842012, Richmond, Virginia 23284, USA;* [2]*Pacific Northwest National Laboratory, Joint Global Change Research Institute, 5825 University Research Ct, College Park, Maryland 20740, USA;* [3]*Department of Natural and Environmental Sciences, Western Colorado University, 1 Western Way, Gunnison, Colorado 81231, USA;* [4]*United States Department of Agriculture Forest Service, Southern Research Station, P.O. Box 700, New Ellenton, South Carolina 29809, USA;* [5]*University of Michigan Biological Station, 9133 Biological Rd, Pellston, Michigan 49769, USA*

Abstract

Soil respiration (R_s) is the largest outward flux of carbon (C) from terrestrial ecosystems, accounting for more than half of total temperate forest C loss. Evaluating the drivers of this globally important flux, as well as identifying autotrophic (R_a) and heterotrophic (R_h) responses, is critical in the era of rapid global change because small changes could result in disproportionally large impacts to ecosystem C balance. We assessed four years of R_s and R_h from the Forest Resilience Threshold Experiment (FoRTE) to better understand how soil C fluxes respond to a disturbance simulating phloem-disrupting insects. This replicated experiment spanning multiple landscape ecosystems contains four disturbance severities of 0, 45, 65 and 85% gross defoliation as well as two disturbance types targeting the upper and lower canopy. We found an immediate and sustained decline in R_s following phloem disruption that persisted for three years and was proportional to severity. Proportional declines in basal soil respiration and fine-root production with increasing disturbance severity and stable R_h lead us to conclude that R_a drove the suppression of R_s into the third year following disturbance. These responses were conserved across four landscape ecosystems, suggesting the mechanisms causing R_s to decline following phloem disruption were similar despite large differences in composition and productivity. The 3-year reduction of C losses through R_s and, contrastingly, sustained C storage through wood production suggests ecosystem C balance may have remained relatively stable in the first few years following disturbance, even at the highest severity.

Key words: carbon; disturbance; ecosystems; phloem disruption; resistance; soil respiration.

Received 4 October 2022; accepted 17 June 2023

Supplementary Information: The online version contains supplementary material available at https://doi.org/10.1007/s10021-023-00863-z.

Author Contributions: KCM performed research, analyzed data, contributed new methods and models and wrote the paper. SP and CR performed research and analyzed data. JWA performed research, analyzed data and contributed new methods. CSV performed research and contributed new methods. BBL and CMG conceived of and designed study, contributed new methods and models and contributed to manuscript writing.

*Corresponding author; e-mail: matheskc@vcu.edu

Published online: 17 July 2023

Highlights

- R_s declined proportionally to disturbance severity following phloem disruption.
- Autotrophic respiration drove sustained declines in R_s for 3-year post-disturbance.
- Contrasts in R_s and production trends suggest sustained C balance even after severe disturbance.

Introduction

Disturbance regimes are changing in North America's upper Great Lakes region (Gough and others 2016) resulting in an uncertain future for terrestrial carbon (C) cycling processes, including soil respiration (R_s, the soil-to-atmosphere CO_2 flux) (Cohen and others 2016; Sommerfeld and others 2018). R_s, the largest terrestrial C efflux, contributes more than half of total temperate forest ecosystem respiration (Binkley and others 2006; Bond-Lamberty and others 2018; Lei and others 2021), and even small disturbance-prompted shifts in this large flux can transition ecosystem C balance from sink to source (Amiro 2001). Regionwide, disturbances caused by pests or pathogens are expanding and becoming more frequent, producing gradients of tree mortality (i.e., *disturbance severity*, sensu (Stuart-Haëntjens and others 2015)) across forested landscapes (Ayres and Lombardero 2000; Flower and others 2013; Seidl and others 2017; Wilson and others 2019). While the immediate effects of severe, stand-replacing disturbances on R_s are well-understood (Frey and others 2006; Hu and others 2017; Dietrich and MacKenzie 2018; Bai and others 2020), longer-term C cycling responses to low-to-moderate disturbance severity gradients are less clear despite their increasing prevalence. Moreover, theory and observations suggest that the components of R_s, autotrophic (R_a) and heterotrophic (R_h) respiration, could respond differently to phloem-disrupting disturbance because these disturbances modify plant and microbial processes through different mechanisms (Harmon and others 2011). Rates of R_a are dependent upon the allocation of recently fixed photosynthate to roots (Högberg and others 2001; Gaumont-Guay and others 2008), whereas R_h is strongly coupled with the quantity of detritus produced through disturbance (Harmon and others 2011; Mayer and others 2017). Because detritus-fueled R_h may determine whether disturbance transitions a system from C sink to source, assessing component fluxes is critical to understanding how disturbances of different severities and sources impact ecosystem C balance (Bond-Lamberty and others 2004).

While gradients of disturbance severity are widespread on forested landscapes, prior observations of R_s focus on single levels of disturbance severity and first-year responses. For example, researchers have used phloem disruption via stem-girdling or chilling as a methodology to examine below-ground processes in the absence of carbohydrate transport, showing major declines in bulk R_s within days or weeks following disturbance (Högberg and others 2001; Bhupinderpal-Singh and others 2003; Binkley and others 2006). While a breadth of literature has produced a robust understanding of R_s response at the highest end of disturbance severity immediately following phloem disruption, R_s responses to phloem disruption over multiple years *and* multiple severity levels are not known. Addressing this knowledge gap is timely and critical because disturbances from phloem-disrupting insects are increasing in Northern American forests (Edgar and Westfall 2022). Patterns of R_s response to other disturbance types, such as fire, herbivory and drought, particularly at moderate severity levels, have been highly variable, with R_s increasing (Zhao and others 2018), decreasing (Sun and others 2014), or remaining the same (Masyagina and others 2006). In addition to the variability present among disturbance types, long-term field experiments and modeling studies suggest soil C cycling processes may be dynamic for years to decades following disturbance (Harmon and others 2011; Cooperdock and others 2020; Xu and others 2022). Therefore, investigating multi-year responses of R_s to a breadth of severities through systematic experimentation is critical to advancing real-world mechanistic understanding of disturbance responses over time (Hicke and others 2012).

We used a large-scale, replicated phloem-disrupting experimental manipulation of disturbance severity and type called the Forest Resilience Threshold Experiment (FoRTE) to characterize 3-year responses in R_s and R_h, focusing on the initial ''resistance'' phase of disturbance response. We define resistance as the initial direction and magnitude of change in functioning, here R_s and R_h, following disturbance *sensu* (Mathes and others 2021). Our specific objectives are to: O1) Characterize 3-year absolute changes in R_s and R_h and quantify normalized R_s and R_h resistance as a function of disturbance severity and disturbance type; O2) Determine whether R_s and R_h respond similarly to disturbance severity and type treat-

ments; O3) Calculate temperature sensitivity of R_s (Q10) and basal respiration rates (BR) and assess whether these metrics change across the disturbance severity gradient and between disturbance types. We hypothesize that: 1) R_s declines will be immediate and proportional to increasing disturbance severity, and correlate with declines in fine-root production; 2) in contrast, R_h will exhibit a lagged and gradual increase with increasing disturbance severity over time as detritus increases; and 3) R_s will decline more in the disturbance type targeting smaller canopy trees because the higher root/shoot in small diameter trees will cause a proportionally larger reduction in root mass and respiration, and thus soil respiration (Ledo and others 2018). We present both absolute and normalized R_s and R_h responses to disturbance treatments because they offer complementary assessments of disturbance response; the former expresses the absolute magnitude of change in fluxes following disturbance, and the latter, an effect size, presents the treatment response relative to a control, allowing for a normalized comparison of fluxes derived and expressed using different methods and units, respectively (Mathes and others 2021).

Methods

Study Site and Experimental Design

Our research site is the University of Michigan Biological Station (UMBS) near Pellston, MI, USA (45.56 N, 84.67 W). The mean annual air temperature and precipitation are 5.5 °C and 817 mm, respectively (Gough and others 2021a). Our study sites are ~ 110-year-old temperate mixed hardwood forests with variation in vegetation types and site productivity attributed to underlying glacial landforms, notably outwash plains and terminal moraines, which create distinct topography, microclimate and soil textures (Pearsall and others 1995). The outwash sites are transitioning from a big-toothed aspen (*Populus grandidentata)* and paper birch (*Betula papyrifera)* dominated canopy to red maple (*Acer rubrum),* Eastern white pine (*Pinus strobus*) and Northern red oak (*Quercus rubra*) dominated canopy and subcanopy. The terminal moraine sites are transitioning from *P. grandidentata* and *B. papyrifera* to sugar maple (*Acer saccharum),* American beech (*Fagus grandifolia)* and striped maple (*Acer pensylvanicum)* dominated canopy and subcanopy. Soils are spodosols ranging from well-drained loam on the more productive moraine landforms to excessively drained sand on the outwash plain (Pearsall and others 1995).

We initiated FoRTE in 2019 to identify the mechanisms underpinning forest C cycling stability across a range of disturbance severities and sources (Gough and others 2021a). While our analysis focuses on soil respiration, prior analyses from FoRTE emphasized aboveground C cycling processes (Grigri and others 2020; Atkins and others 2021; Niedermaier and others 2022), modeled responses to the FoRTE treatments (Dorheim and others 2022) and structural and compositional change (Gough and others 2021a), with a key finding demonstrating that C uptake and allocation to biomass was sustained in the first 3 years after disturbance, even at the highest severity level (Grigri and others 2020; Gough and others 2021a; Niedermaier and others 2022). Following pre-disturbance data collection in 2018, we stem girdled a total of ~ 3600 canopy trees (> 8 cm diameter at breast height, DBH) in May 2019. The girdling treatment was implemented by scoring the full circumference of each stem twice, 15–20 cm apart, with a chainsaw through the phloem tissue. The bark and phloem tissues between the circular cuts were then removed using a pry bar. The experiment was replicated in four different ecosystem types that are representative of upper Great Lakes regional variation in forest productivity, plant community composition, topography and soil microclimate (Nave and others 2019; Gough and others 2021a). Notably, the four treatment replicates are positioned on ecosystems spanning a twofold range in biomass and a threefold range in canopy complexity (Table 1).

Each replicate was comprised of four 0.5 ha circular whole plots (n = 16) randomly assigned to target levels of gross defoliation, i.e., disturbance severity of 0% (control), 45%, 65% or 85% determined from tree allometric equations. Each whole-plot was split into two, 0.25 ha split-plots (n = 32) and randomly assigned a disturbance type affecting the canopy from the ''top-down'' or ''bottom-up'' (Atkins and others 2020). In the ''top-down'' treatment, the largest DBH tree within a subplot was girdled first, regardless of species, followed by sequentially smaller trees until the targeted severity (i.e., gross defoliation) level was reached. ''Bottom-up'' treatments, conversely, followed ascending DBH (> 8 cm) order (Figure 1A: FoRTE map). These treatment types simulate the structural outcomes of disturbance agents targeting larger and smaller tree size classes, respectively (Atkins and others 2020). One circular 0.1 ha

Table 1. Vegetation Characteristics, Landforms and Soil Textures of Treatment Replicates in the Forest Resiliencece Threshold Experiment (FoRTE) Before Disturbance Severity and Type Treatments Were Implemented (2018)

	A	B	C	D
Canopy tree (> 8 cm DBH) composition	POGR (61%) ACSA (17%) ACRU (10%) FAGR (10%)	POGR (58%) ACRU (24%) QURU (9%) FAGR (4%)	QURU (43%) POGR (39%) PIST (6%) ACRU (6%)	QURU (72%) POGR (19%) PIST (4%) FAGR (1%)
Stem density (Stems ha^{-1}, > 8 cm)	865 (32)	888 (46)	910 (55)	796 (81)
Shannon's index of species diversity	1.05 (0.09)	1.05 (0.05)	1.04 (0.11)	0.92 (0.10)
Leaf area index (dimensionless)	4.1 (0.15)	3.6 (0.08)	3.5 (0.10)	2.9 (0.18)
Biomass (kg C ha^{-1})	264,6000 (15,800)	229,900 (24,700)	197,000 (13,900)	155,900 (19,000)
Canopy rugosity (m)	28.8 (3.6)	22.3 (2.3)	14.2 (1.7)	8.9 (1.1)
Landform	Moraine	High-elevation outwash over moraine	High-elevation outwash plain	High-elevation outwash plain
Soil Texture	Sandy loam, calcareous	Medium sand, non-calcareous	Sand, calcareous	Sand, calcareous
Drainage	Well-drained	Well-drained	Excessively drained	Excessively drained

Species abbreviations are as follows: POGR (Populus grandidentata), ACSA (Acer saccharum), ACRU (Acer rubrum), FAGR (Fagus grandifolia), QURU (Quercus rubra), PIST (Pinus strobus).

subplot was nested in each disturbance severity x type treatment split-plot (n = 32).

Aboveground Biomass and Vegetation Area Index (VAI)

Total aboveground wood biomass was calculated from a full census of canopy trees in all subplots during summer of 2018. DBH was measured for all trees > 8 cm using a tape, and biomass was calculated using species and site-specific allometric equations (Gough and others 2021a). Allometries were also used to estimate the projected leaf area of each censused tree and to assign girdled or ungirdled status to each individual to achieve targeted levels of 0, 45, 65 and 85% gross defoliation and the ''top-down'' and ''bottom-up'' treatments.

To evaluate changes in canopy structure following disturbance, we annually sampled the vegetation area index (VAI) of each subplot using LiDAR during peak leaf out. VAI is conceptually similar to LAI, but additionally includes lateral branches. A complete description of VAI determination is detailed in Gough and others (2022); briefly, we employed a terrestrial portable canopy LiDAR (PCL) system that uses an upward-facing pulsed laser to map the location and density of vegetation. Raw LiDAR hit data were binned into horizontal and vertical grids, and VAI was estimated using the *forestr* package (Atkins and others 2018). VAI was sampled in each of the 32 subplots once a year during peak growing season from 2018 to 2021.

Bulk Soil Respiration (R_s) and Soil Micrometeorology

We measured in situ bulk soil respiration (R_s, $\mu molCO_2\ m^{-2}\ s^{-1}$) for four years, one year prior and three years following disturbance. Four measurement campaigns were taken before disturbance, between July 2018 and May 2019, and 14 were taken between May 2019 and November 2021, after the stem-girdling disturbance was implemented. Each of the 32 subplots contained five permanent, 10-cm-diameter PVC collars, for a total of 160 collars experiment-wide, installed 4-cm deep and leaving 1 cm above the soil surface. Collars positioned along opposite cardinal axes were spaced 10 m apart, with one additional collar installed at the subplot center (Figure 1B). R_s measurements were made at every collar 3 to 7 times a year using a LI-6400 portable gas analyzer with a 10-cm-diameter cuvette (LI-COR Inc, Lincoln, NE, USA). At each measurement location, two R_s values were recorded and averaged for analysis. Measurement campaigns were completed within three days under climatologically similar conditions. The settings during measurements were

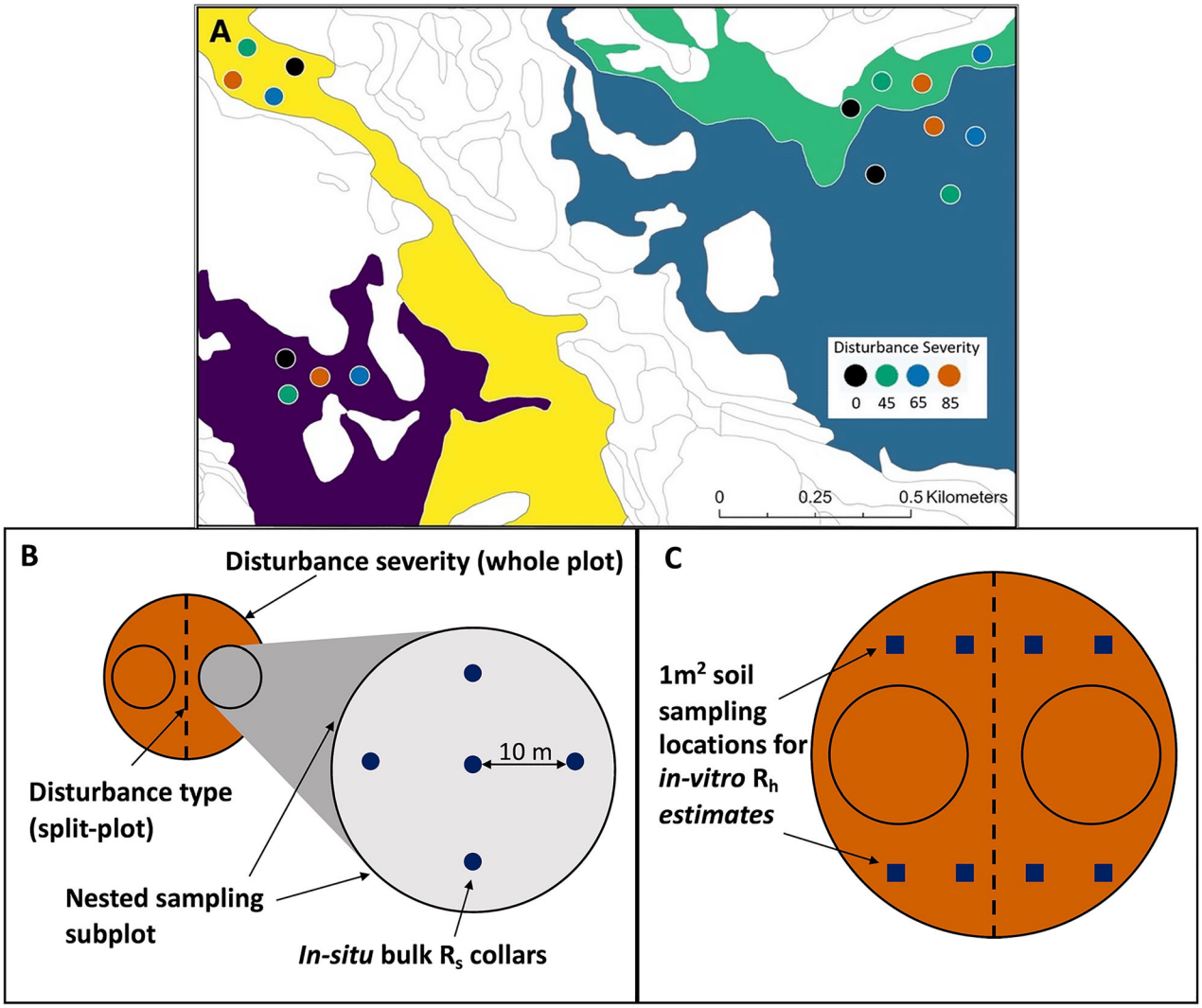

Figure 1. Forest resilience threshold experiment (FoRTE). **A** plot distribution map, **B** experimental design and layout of in situ bulk soil respiration (R_s) collars and **C** layout of soil sampling locations for in vitro heterotrophic respiration (R_h) estimates.

as follows: 400 ppm target CO_2 concentration with measurement range from 390 to 410 ppm (delta = 10), 10 s gap between drawdown and measurements (Dead Time), 20 s minimum measurement time, 120 s maximum measurement time, 80 cm^2 soil surface area within chamber, 50–200 (µmol s^{-1}) drawdown flow rate during dormant season measurements and 200–500 (µmol s^{-1}) drawdown flow rate during growing season measurements. To minimize the confounding of treatment and time-of-day, subplot sampling order within a replicate, as well as order of the replicates, were randomized for each measurement campaign. R_s measurements were not taken within 24 h of heavy precipitation. R_s measurements were paired with adjacent measurements of 7-cm depth soil temperature (T_s, °C) using a LI-6400 thermocouple probe and 20-cm integrated soil volumetric water content % (VWC) using a CS620 soil moisture probe (Campbell Scientific, Inc, Logan, UT, USA).

Soil Heterotrophic Respiration (R_h)

The heterotrophic respiration of surface soils (R_h, µmol CO_2 g^{-1} s^{-1}) was estimated from incubated root-free soils (Curtis and others 2005) using a method previously applied at our site and shown through independent cross-validation to produce ecologically plausible values (Mathes and others 2021). Soils were collected from four, 1 m^2 sampling squares located on the north and south ends of each subplot margins (n = 128 experiment-wide; Figure 1C) annually between 2019 and 2021.

Once a year in July or August, soils from each sampling location were excavated to 10-cm depth, excluding the freshest litter layer (O_i horizon) but including partially and fully decomposed organic layers (O_e and O_a horizons) and A horizon. Soils were collected with a 10-cm-diameter metal corer from three randomly selected points within each 1 m^2 sampling location and then pooled and manually homogenized. T_s at 7-cm depth was measured concurrently. Immediately following collection, soils were refrigerated at 4 °C for 24 h, sieved to remove roots and fragments, and root-free soil placed in a 950 cm^3 glass jar, leaving 350 cm^3 of headspace. Soil filled glass jars were weighted, capped with a 1-mm ventilation hole and incubated for 2 weeks at the average T_s recorded within a replicate on the day of collection, which ranged from 14.8 to 21.6 °C. Following incubation, unadjusted CO_2 efflux (μmol CO_2 m^{-2} s^{-1}) was measured with a LI-6400 portable gas analyzer (LI-COR Inc, Lincoln, NE, USA) and custom cuvette system fitted to soil filled glass jars. Prior to measurements, we degassed soils on a benchtop by removing the jar lid for 75 min (Figure S1). Next, four sequential CO_2 efflux measurements were taken per soil filled jar and the last two were retained for analysis to ensure stability. We then dried a soil subsample from each jar at 60 °C for 48 h to determine soil dry mass (g). R_h (μmol CO_2 g^{-1} s^{-1}) was estimated by converting fixed area-based efflux measurements (μmol CO_2 m^{-2} s^{-1}) to soil sample-specific dry mass-adjusted estimates of R_h.

R_s Temperature Response Curves (Q10 and Basal R_s Rates)

To quantify R_s temperature response curves, we used a two-parameter exponential equation model fit separately to data from each subplot (Eq. 1, (Meyer and others 2018) and interpreted temperature sensitivity from Q10 values (Eq. 2) and basal R_s rates (BR) at 10 °C). We analyzed differences between average Q10 values and BR across disturbance severities and between disturbance types.

$$Rs_t = a * \exp^{b*T_s} \quad (1)$$

$$Q10 = \exp^{b*T_s} \quad (2)$$

Annual Fine-root Production

We measured fine-root production annually from 2019 to 2021 using root in-growth cores installed at the beginning of each growing season (May–June) and extracted at the end of the growing season (November). Four, 5-cm-diameter hard plastic, 2-mm mesh cores were installed to 30-cm soils depth in each subplot (n = 128) and were 1-m away from paired R_s collars. Cores were filled with sieved soils from adjacent forest plots with physical and chemical properties comparable to those found in the FoRTE plots (Pearsall and others 1995). Extracted cores were stored at 4 °C until processing. The four cores from each subplot were pooled and homogenized, and then sieved to remove roots, washed, dried at 60 °C for 48 h and weighed to determine dry mass. To adjust for ash-free mass, twelve roots were subsampled, burned in a muffle furnace at 500 °C for 12 h, and a common ash-free adjustment of 97% was applied to all samples. Root production was scaled and converted to carbon mass (kg C m^{-2} y^{-1}) using a site-specific C fraction of 0.49 (Gough and others 2008).

Quantifying R_s and R_h Resistance Values

To compare normalized measures of R_s and R_h resistance, we adopted a framework described in Mathes and others (2021) and Hillebrand and others (2018) (Eq. 3). This approach allows us to directly compare patterns and changes in fluxes with variable units and magnitudes that may be obscured when only assessing absolute values. Resistance is a dimension of stability quantitatively describing the magnitude of initial response to disturbance normalized against a control and expressed on a natural log scale.

$$\text{resistance} = \ln\left(\frac{\text{Disturbance } R_x}{\text{Control } R_x}\right) \quad (3)$$

where *Disturbance* R_x is the respiratory flux (R_s *or* R_h) in a disturbed plot or sample and *Control* R_x the respiratory flux in the control plot or sample. *Resistance* values that are < 0 represent a respiratory (i.e., functional) decline relative to the control, *resistance* values = 0 represent no change, and *resistance* values > 0 represent functional increase.

Statistical Analysis

Analysis of Absolute Values

To analyze the effect of disturbance severity and type on R_s and R_h (O1 and O2), we used a repeated measures split-split plot fully replicated ANOVA model with alpha values set to 0.05 (Gough and others 2021a). We used replicate (i.e., landscape ecosystem) as the blocking factor, disturbance severity as the whole-plot factor, type as the split-plot factor and year as the split-split plot factor. We

tested models with VWC and T_s as covariates and chose the best fit model based on the Akaike information criterion (AIC). The best fit model for R_s included neither T_s nor VWC as covariates and for R_h included untransformed VWC as a covariate. All model assumptions were met without transformation for R_s and with a log transformation of R_h data. To minimize spatial auto-correlation, the experimental unit was the subplot average over 5 collars for R_s and the subplot average over the 4 soil sampling plots for R_h. Pairwise analyses (alpha = 0.05) were performed on all significant main effects and interaction using Fisher's least significant difference (LSD) test (See Tables S1 and S2 for full ANOVA models and post hoc output). Interactions were only included in post hoc analyses if at least one component main effect was significant and there were a priori ecological expectations.

To analyze the effect of disturbance severity and type on the Q10 and BR values for the temperature sensitivity of R_s (O3), we ran the same split-plot, fully replicated ANOVA as described above, except year was not included in the model (See Tables S3 and S4 for full ANOVA models and post hoc output). Finally, the same split-split plot ANOVA was also run to characterize VAI response to disturbance severity and type over time. (See Tables S5 for full ANOVA models and post hoc output). All analyses were performed in R (R Core Team 2022), the split-split plot ANOVA design was made in the package ''stats'' (R Core Team 2022), the LSD test was conducted using the package ''agricolae'' (de Mendiburu 2021), and all figures were made in the package ''ggplot2'' (Wickham 2016).

To analyze the relationship between R_s and annual fine-root production, we ran a multivariate linear regression analysis with R_s as a function of fine-root production, disturbance severity and time (year). Severity and time were included as covariates to assess whether the relationship changed over time and was different across the severity treatments. All model assumptions were met with a log transformation of fine-root production. Pairwise analyses of significant interactions were preformed using Tukey's honestly significant difference (HSD) test to compare slopes of R_s as a function of fine-root production across severities (See Tables S6 for regression and post hoc output). Multiple linear regression was performed using R package ''stats'' (R Core Team 2022), and Tukey's HSD tests were performed using package ''emmeans'' (Lenth 2022).

Analysis of R_s and R_h Resistance Values

To quantify the relationship between R_s and R_h resistance and disturbance severity (O1 and O2), we conducted multiple linear regression analyses with R_s or R_h resistance as a function of severity and time (year), and regression analysis and post hoc test were performed as described above. All model assumptions were met without transformation (See Tables S7 and S8 for regression and post hoc output).

Results

Aboveground Biomass and Vegetation Area Index (VAI)

The amount of remaining ungirdled biomass following the treatment implementation was generally proportional to the targeted treatment levels of gross defoliation (i.e., disturbance severity) (Figure 2A). In contrast, declines in VAI with increasing disturbance severity lagged girdling and were not directly proportional in magnitude (i.e., 1:1) to gross defoliation (Figure 2B) because of the gradual rate of mortality and associated defoliation that occurs following phloem disruption (Stuart-Haëntjens and others 2015). Significant differences in VAI emerged in 2019 between the control and at 85% severity but were not present among all severities until 2021 (Figure 2B; $F = 2.045$, $p = 0.47$).

Seasonality and Range of Soil Respiration (R_s) and Microclimate Data

Across all disturbance treatments, mean R_s, T_s and VWC values varied seasonally and were within the range of previously recorded values from our site (Clippard and others 2022). Mean subplot R_s varied by more than an order of magnitude, from 0.5 to 14.3 μmol CO_2 m^{-2} s^{-1}, with low values occurring during the cooler dormant season. Summertime T_s ranged from 10.1 and 24.7 °C, declining to an average of 4.2 °C during the dormant season. VWC displayed the opposite seasonal pattern, reaching high values of 22% during the dormant season and minimum values as low as 3% during the summer (Figure 3). Pre-treatment (2018) control R_s was significantly lower than subsequent years, which was driven by low summertime VWC (Figure S2).

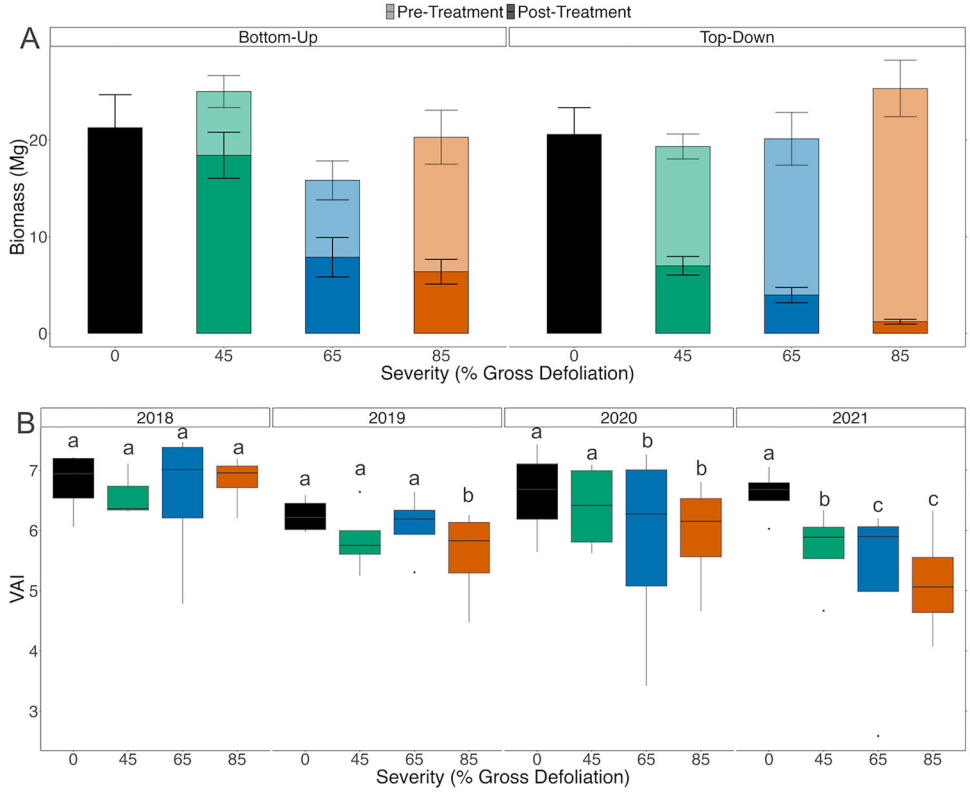

Figure 2. **A** Mean aboveground wood biomass ± SE by disturbance severity and disturbance type prior to girdling in 2018 (whole bar) and remaining ungirdled biomass following disturbance treatment applications in 2019 (solid shade only). **B** Median, interquartile range (middle 50% of range) and minimum and maximum vegetative area index (VAI) values by disturbance severity for pre-disturbance (2018, gray shading) and post-disturbance (2019–2021) years. Different letters indicate significant within-year differences among disturbance severities (alpha = 0.05, $F = 2.045$, $p < 0.047$).

Soil Respiration (R_s) and Disturbance Severity

A pattern of declining R_s with increasing severity emerged the year of the girdling disturbance (2019) and persisted for three consecutive years (Figure 4). Declines in R_s were temporally aligned with the onset of the girdling and proportional to the targeted levels of gross defoliation (Figure 2A), but preceded declines in total VAI across all severities by two years (Figure 2B). We did not observe differences among disturbance severity treatments prior to girdling in 2018. However, the girdling treatment in 2019 prompted a significant decrease in R_s with increasing severity, and this pattern held through 2021 ($F = 4.42$, $p < 0.001$). From 2019 to 2021, control R_s values were consistently higher than those observed in the disturbance severity treatments, with mean R_s in the 85% disturbance severity treatment averaging 35% less than the control (Figure 4).

Soil Respiration (R_s) and Disturbance Type

In contrast to disturbance severity, we observed no significant differences in R_s between top-down and bottom-up disturbance types before (2018) or after (2019–2021) stem girdling (Figure 5). Within-year pairwise treatment comparisons revealed no significant differences ($F = 0.924$, $p = 0.42$), indicating that the stem size distribution of girdled trees had no effect on R_s in the first three years following disturbance.

R_s Temperature Response Curves, Q10 and Basal *R*s Rates

The step-down pattern of R_s with increasing disturbance severity was caused by a reduction in basal soil respiration (BR) rather than change in temperature sensitivity. Post-disturbance R_s exhibited similar exponential increases with temperature (i.e., temperature sensitivities) across disturbance severities ($F = 1.847$, $p = 0.21$, Figure 6A, C) and disturbance types ($F = 1.343$, $p = 0.27$, Figure 6B,

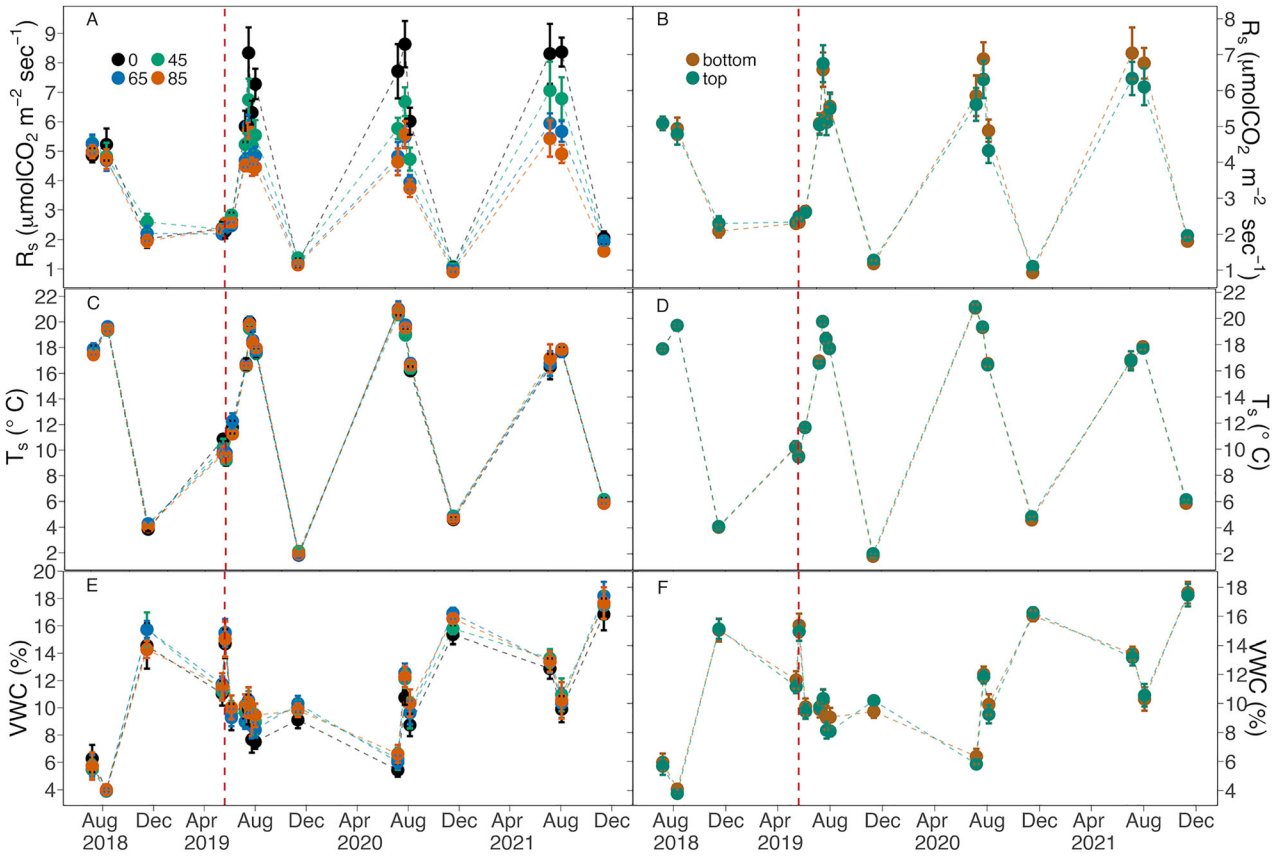

Figure 3. Mean (± 1 S.E.) discrete measurements of soil respiration (R_s; **A**, **B**), soil temperature (T_s; **C**, **D**), and volumetric water content (VWC; **E**, **F**) by disturbance severity (left panels) and disturbance type (right panels), 2018–2021. Red vertical dashed line delineates pre- and post-disturbance measurement periods.

D), with Q10 averaging 2.24. However, BR and R_s displayed similar significant declines ($F = 4.418$, $p = 0.04$, Figure 6E) with increasing disturbance severity, from 3.59 to 2.42 μmol CO_2 m^{-2} s^{-1} at 10 °C, and was similar between the top-down and bottom-up treatments ($F = 0.17$, $p = 0.690$, Figure 6F).

Heterotrophic Respiration (R_h) and Disturbance Severity and Type

Mean R_h was the lowest in the 65% disturbance severity and top-down treatments, departing somewhat from the trends of total R_s. R_h ranged from 0.0017 to 0.012 μmol CO_2 g^{-1} s^{-1} with a grand mean of 0.004 μmol CO_2 g^{-1} s^{-1} between 2019 and 2021. R_h was significantly lower in the 65% treatment (Figure 7A , F= 4.369, $p = 0.042$), and we did not find a year x treatment interaction, indicating that the relationship between R_h and disturbance severity was consistent across years. A significant but quantitatively small difference of 8.7% between the top-down and bottom-up treatments was also present following disturbance (Figure 7B , $F = 6.837$, $p = 0.024$); however, the difference was too small and noisy to significantly influence total R_s.

Fine-root Production and R_s

We observed a significant positive relationship between R_s and fine-root production in stem-girdled but not control plots (Figure 8, $R^2 = 0.50$, p-value < 0.001). The slope of the fine-root production–R_s relationship did not differ among post-disturbance years or levels of disturbance severity. However, the slopes of control and disturbance plots (all severities) were significantly different (Figure 8, $F = 2.2$, p-value = 0.03), suggesting disturbance-induced declines in fine-root production drove reductions in R_s.

Soil Respiration (R_s and R_h) Resistance

A comparison of normalized R_s and R_h resistance values underscores their contrasting relative response to increasing disturbance severity, further

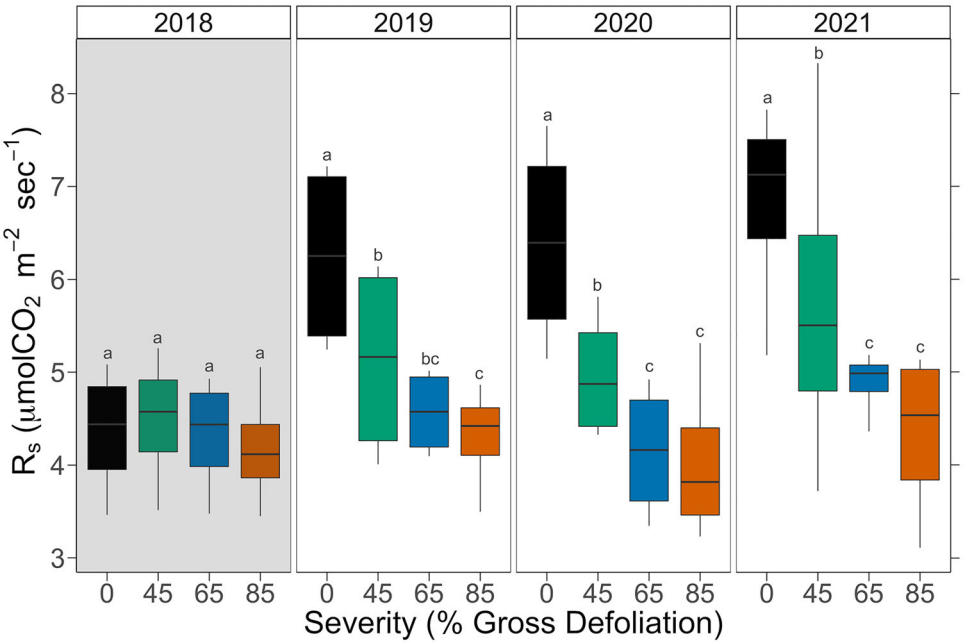

Figure 4. Boxplots displaying median, interquartile range (middle 50% of range) and minimum and maximum soil respiration (R_s) values by disturbance severity for pre-disturbance (2018, gray shading) and post-disturbance (2019–2021) years. Different letters indicate significant within-year differences among disturbance severities (alpha = 0.05, $F = 4.42$, $p < 0.001$).

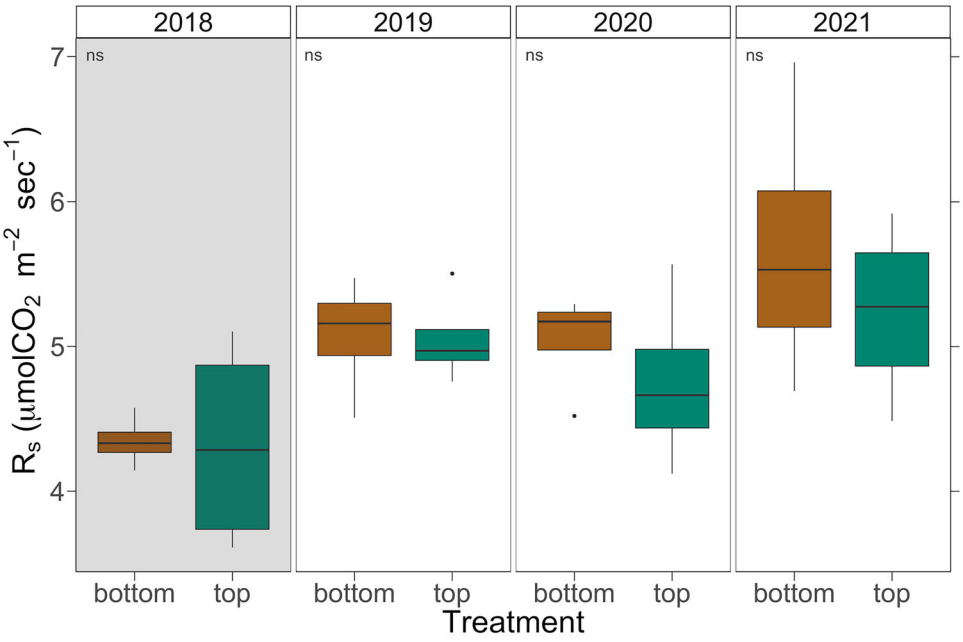

Figure 5. Boxplots displaying median, interquartile range (middle 50% of range) and minimum and maximum soil respiration (R_s) values by ''top-down'' and ''bottom-up'' disturbance types for pre-disturbance (2018, gray shading) and post-disturbance (2019–2021) years. Within-year comparisons yielded no significant differences (alpha = 0.05, $F = 0.942$, $p = 0.42$).

suggesting that autotrophic rather than heterotrophic respiration primarily drove declines in total soil CO_2 efflux. R_s resistance exhibited a temporally consistent decline across the disturbance severity gradient following stem girdling from 2019 to 2021, showing as much as 37% decrease in the highest

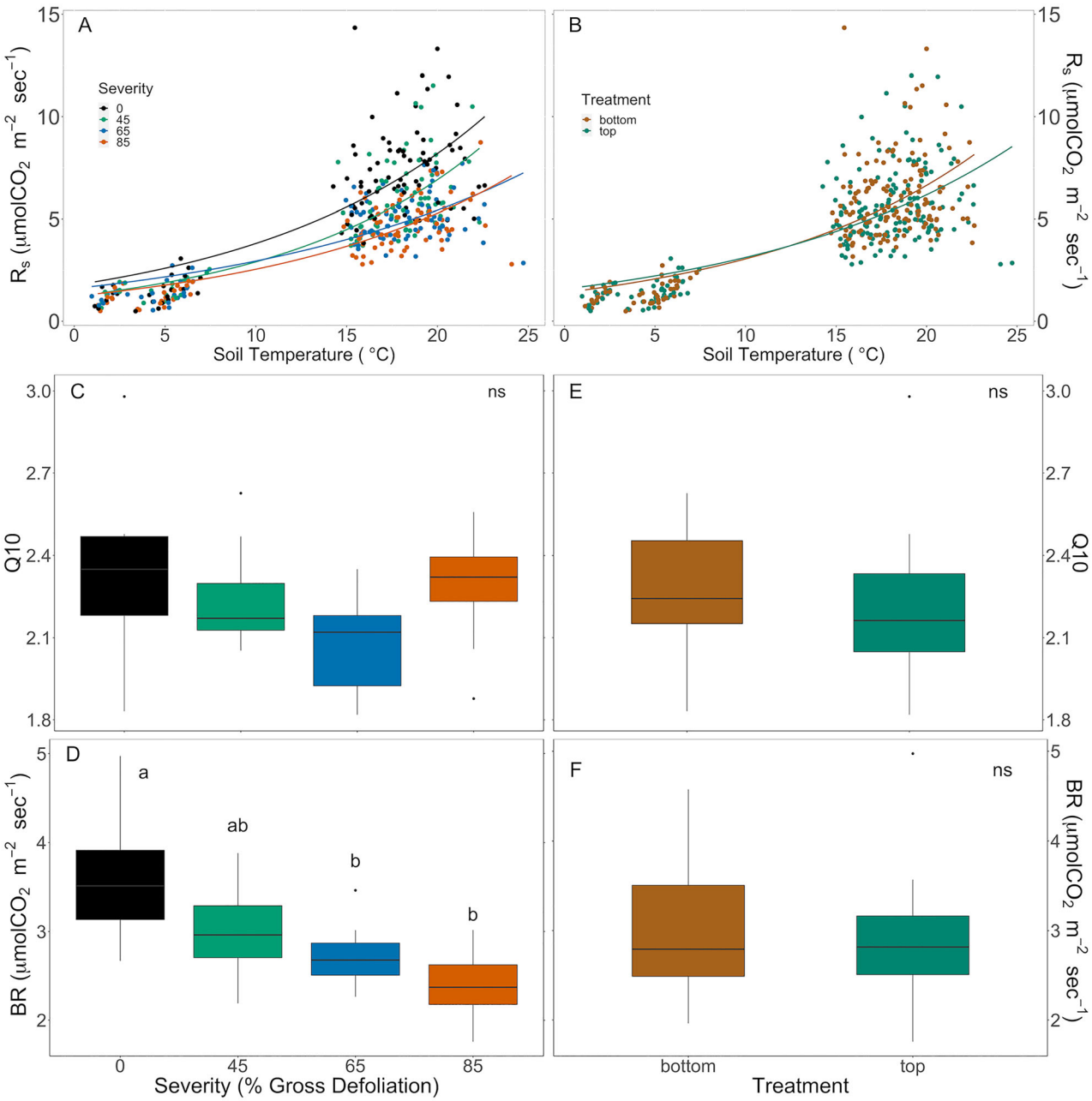

Figure 6. Post-disturbance (2019–2021) relationship between soil temperature and R_s using a two-parameter exponential model by **A** disturbance severity (0, 45, 65 and 85% gross defoliation) and **B** by disturbance type (''top-down'' and ''bottom-up''). Average Q10 values (increase in R_s for every 10 °C in T_s) by **C** Disturbance severity ($F = 1.847$, $p = 0.21$) and **D** disturbance type ($F = 1.343$, $p = 0.27$). Average basal R_s rates (BR) at 10 °C by **E** Disturbance severity ($F = 4.418$, $p = 0.04$) and **F** Disturbance type ($F = 0.17$, $p = 0.690$).

severity as compared to the control (Figure 9A). Contrastingly, R_h resistance, while variable, did not change significantly across disturbance severity treatments (Figure 9B), only showing a 7% decline in the highest severity. This result suggests that 3-year declines in R_s primarily were driven by consistently suppressed autotrophic respiration.

Discussion

Our analysis provides new mechanistic insight into how forest R_s responds to a range of disturbance severities caused by phloem disruption. With complementary analyses of absolute measurements and normalized resistance values, we observed an immediate and strikingly sustained 3-year decline

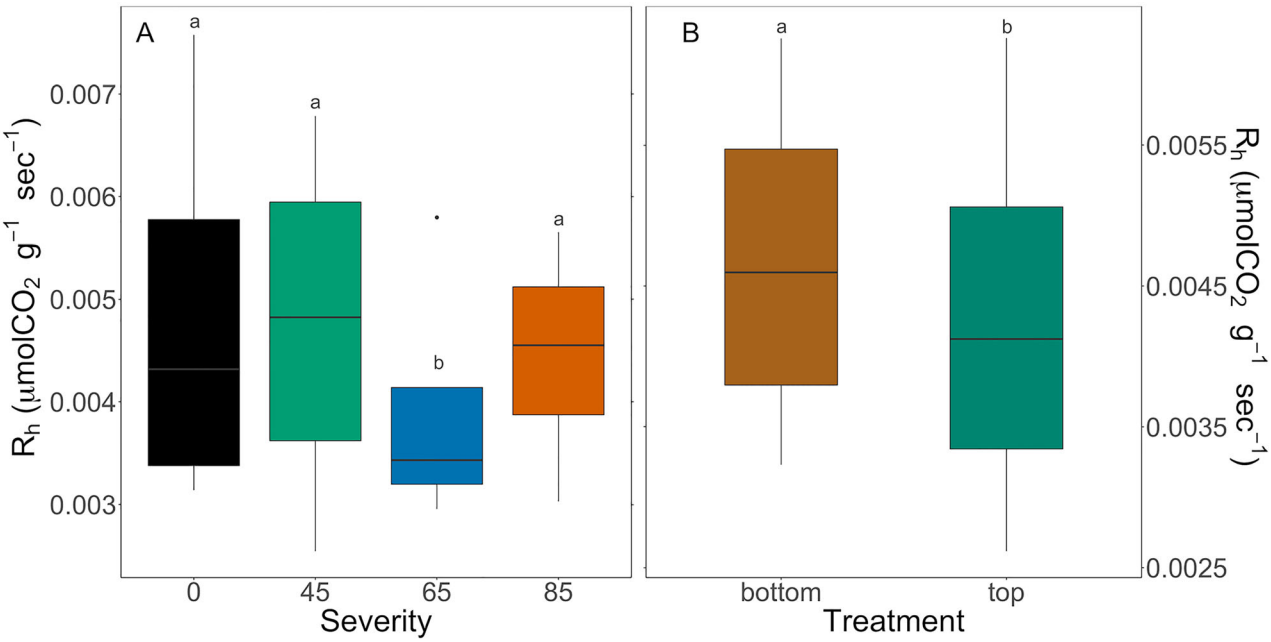

Figure 7. Boxplots displaying median, interquartile range (middle 50% of range) and minimum and maximum soil heterotrophic respiration estimates (R_h) of incubated root-free soils (10 cm depth) averaged across all post-disturbance years (2019–2021) by: **A** disturbance severity (alpha = 0.05, F = 4.369, p = 0.042) and **B** ''top-down'' and ''bottom-up'' disturbance type (alpha = 0.05, F = 6.837, p = 0.024). Different letters indicate significant differences among disturbance severities or disturbance type.

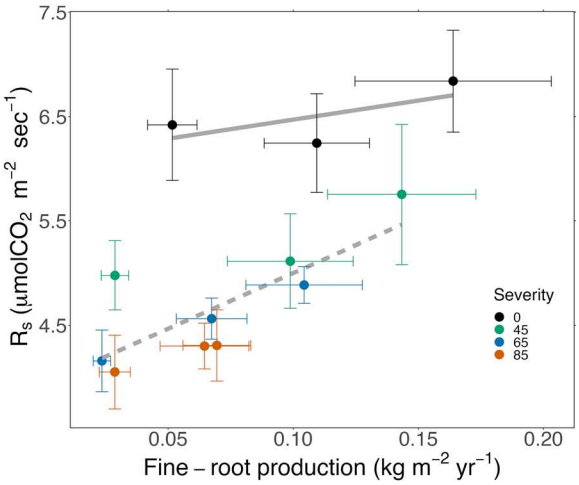

Figure 8. Average R_s as a function of fine-root production, 2019–2021 (p-value < 0.001, Adjusted R^2 = 0.50). Solid gray line represents linear relationship between R_s and fine-root production in the control and dotted gray line represents linear relationship between R_s and fine-root production across disturbance severities. Slopes of the two lines are significantly different from each other (T-value = 2.24, p-value = 0.03).

in R_s with increasing disturbance severity, indicating that disturbance effects were relatively long-lasting and proportional to targeted gross defoliation levels but lagged behind changes in VAI. The temporal mismatch in R_s and VAI responses to girdling was likely associated with the immediate elimination of photosynthate allocation to roots (Högberg and others 2001), but slower and more gradual defoliation. Basal soil respiration (BR), but not R_h or Q10, decreased with increasing disturbance severity and declines in fine-root production drove declines in R_s, suggesting that a reduction in autotrophic rather than heterotrophic respiration or temperature sensitivity drove R_s responses to phloem disruption. In contrast to disturbance severity, the top-down and bottom-up disturbance types exhibited comparable R_s. These findings extend knowledge derived from short-term (for example, 1-year) observations and studies encompassing a narrower range of disturbance severities or forest types (Högberg and others 2001; Nave and others 2011; Bloemen and others 2014), demonstrating that the targeted disturbance severity consistently reduced R_s through its sustained, proportional effect on autotrophic respiration.

Our results indicate that declines from phloem disruption are generally proportional to the degree of disturbance severity expressed as gross defoliation and similar across disturbance types, a finding that contrasts with the response of aboveground production. Our observation that phloem-disrupt-

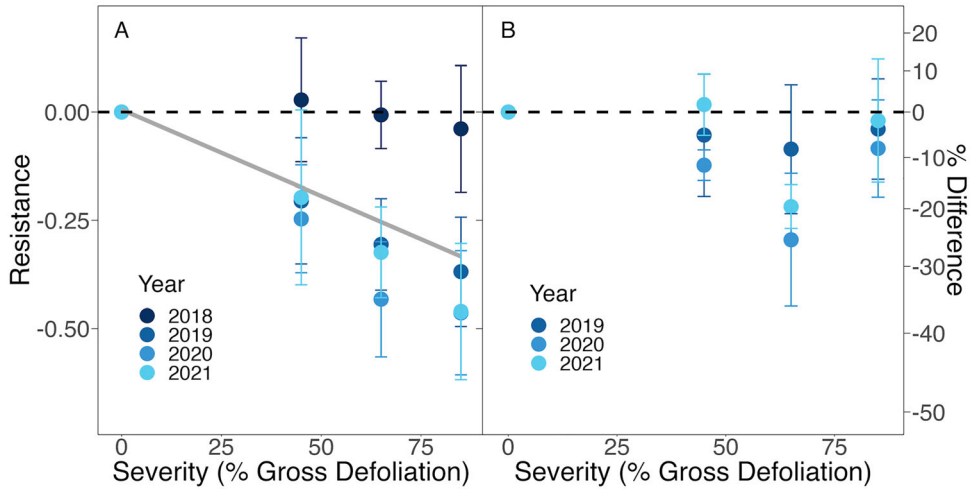

Figure 9. **A** Average R_s resistance and **B** Average R_h resistance as a function of disturbance severity (% gross defoliation), 2018–2021. Gray line indicates significant linear decline in R_s resistance with increasing disturbance severity between 2019 and 2021 (p-value: < 0.001, Adjusted $R^2 = 0.93$). No significant relationship between R_h resistance and disturbance severity.

ing disturbance initially reduces R_s is consistent with numerous studies conducted in a variety of forest types (Bhupinderpal-Singh and others 2003; Andersen and others 2005; Sommerfeld and others 2018; Frey and others 2006; De Schepper and others 2011). Similar to our results, a pattern of declining R_s with increasing tree mortality was observed in a north temperate forest manipulated via stem-girdling (Levy-Varon and others 2012). Additionally, our findings align with studies that report declines in R_s are greater from severe disturbance caused by fire (Kelly and others 2021) and harvesting (Bai and others 2020). Building on these studies, our replicated experiments further demonstrate that patterns of declining R_s with increasing disturbance severity are consistent among forest ecosystems varying substantially in composition, productivity, soils, and landform. Such consistency across ecosystems suggests that a common physiological basis underlies changes in R_s following phloem disruption, regardless of tree species composition. Notably, we did not observe signs of recovery in R_s over time despite finding increases in subcanopy growth and relatively stable total aboveground primary production (Grigri and others 2020; Niedermaier and others 2022). The opposing responses of C uptake (i.e., primary production) and loss (i.e., R_s) suggest that surviving vegetation may have invested less in metabolically active fine root biomass as competition for limiting resources declined after disturbance (Bae and others 2015; Kang and others 2016).

Declines in R_s emerged within the first two months of phloem disruption and persisted through the third year, underscoring a rapid and sustained disturbance response. This rapid R_s response to phloem disruption is consistent with experiments observing almost immediate changes in soil CO_2 efflux after disturbance (Scott-Denton and others 2006; Subke and others 2011). Additionally, our 3-year analysis demonstrates that disturbance effects can persist for years, a duration that is consistent with a landscape-level single severity phloem-disrupting disturbance at our site (Gough and others 2021b), model simulations of the FoRTE treatments (Dorheim and others 2022), and the 6-to-7-year recovery time following a phloem-disrupting insect disturbance elsewhere (Moore and others 2013). However, this sustained decline is longer than the 1-year recovery in R_s following experimental stem-girdling in a temperate deciduous forest (Levy-Varon and others 2014). Simulations of the FoRTE disturbance suggest that climatic and biotic variables such as precipitation, humidity and forest productivity influence the pattern and timing of C cycling disturbance response (Dorheim and others 2022). In contrast, our observations demonstrate that landscape ecosystems with primary production values varying by a factor of four (Gough and others 2021a) exhibit similar initial responses to disturbance.

Our analysis suggests autotrophic rather than heterotrophic respiration predominantly drove declines in R_s following phloem disruption. Girdling immediately eliminates photosynthate trans-

port to roots causing declines in root metabolism and, consequently, R_s (Högberg and Högberg 2002; Chen and others 2010). While we expected to observe a gradual rise in R_h as root detritus increased (Subke and others 2011), three lines of evidence instead point to a sustained 3-year reduction in autotrophic respiration. First, R_h declined slightly or was stable with increasing severity during the three years following disturbance, implying that disturbance-fueled decomposition was minimal, or that it was offset by reduced heterotrophic respiration of root exudates. In contrast, studies of stand-replacing disturbances reveal that a large and rapid influx of organic substrate (Ekberg and others 2007) and extreme shifts in soil microclimate (Mayer and others 2017) can cause immediate increases in R_h. Relatively stable R_h during the first three years of our experiment could suggest that unlike stand-replacing events, the amount of disturbance-induced substrate was not significant enough to cause an immediate microbial priming effect. Furthermore, because declines in VAI lag the onset of phloem-disrupting disturbances, microclimatic changes that may impact R_h were not as pronounced. Our results are consistent with the lagged increase in R_h predicted by model runs of the FoRTE study (Dorheim and others 2022) and by theory (Harmon and others 2011). Second, declines in R_s with increasing disturbance severity were accompanied by parallel reductions in basal respiration (BR) rather than temperature sensitivity (Q10), implying labile rather than more recalcitrant C substrate limited total R_s after stem-girdling. BR rates are particularly sensitive to changes in labile C supply, including the quantity of recently fixed non-structural C allocated to roots, while temperature sensitivity is generally more limited by the degree of organic matter recalcitrance (Bhupinderpal-Singh and others 2003; Sampson and others 2007; Yan and others 2021). Finally, consistent with studies showing declines in fine-root production in windthrow (Ivanov and others 2022) and fire disturbances (Yuan and Chen 2013), variation in fine-root production was a predictor of R_s in the disturbed plots but not the control, suggesting loss of autotrophic activity drove declines in R_s following phloem disruption. Our findings offer useful empirical support for models, theory, and short-term studies, suggesting that the influence of phloem disruption on the autotrophic component of respiration can be long-lasting, despite an imminent influx of disturbance-generated detritus.

Contrary to our hypothesis, we found no significant differences in R_s between disturbance types targeting either upper or lower canopy trees. We anticipated higher root/shoot in smaller stems (Ledo and others 2018) would result in a proportionally greater effect on autotrophic fluxes in the bottom-up treatment. Instead, we observed a small, but significant, increase in R_h in the bottom-up treatment, suggesting that greater fine-root mortality could be gradually enhancing R_h and offsetting the reduction in autotrophic contributions (Ekberg and others 2007). Moving forward, we expect canopy structural changes, which lag behind phloem disruption (Gough and others 2021b), and will impart different effects on soil microclimate in the top-down and bottom-up disturbance types, causing R_s to diverge over the long-term. That top-down and bottom-up disturbance types have not diverged in the first three years following disturbance, in advance of peak canopy structural changes, highlights the need for long-term observations of disturbance response (Buma 2015).

Expressing R_s and R_h responses to disturbance in relative terms (i.e., as resistance) made these fluxes—expressed in different units and spanning a large absolute range—more comparable, while revealing some limitations. Mathes and others (2021) recommended the use of relative, normalized, and systematic expression of disturbance response as a way of placing functional responses derived via different approaches and expressed using different units on equivalent scales. In our study system, we anticipated large absolute differences in fluxes among the different landscape ecosystems. However, a surprisingly uniform response to disturbance across landscape ecosystems varying substantially in productivity, composition, and soils made such normalization less imperative to revealing trends. Nevertheless, the adoption of normalized approaches to characterizing disturbance response may prove useful when magnitudes of response are different or when comparing functional responses across disparate sites, experiments, and biomes (Hillebrand and others 2018; Mathes and others 2021).

Finally, we acknowledge several study limitations. First, the rapid implementation of our disturbance experiment does not simulate the more temporally gradual effects of phloem-disrupting insects (Duan and others 2022). In addition, many prevalent phloem-disrupting insects are host-specific (Busby and Canham 2011; Borkhuu and others 2015) and species-specific physiology, functional traits and evolutionary mechanisms of resistance might become important factors driving functional responses in some circumstances (Seidl and others 2017). However, that we observed

consistent disturbance responses across four different landscape ecosystems suggests severity was a more important driver of R_s than the composition of disturbed individuals. Additionally, the spatial distribution of tree mortality is often affected by tree vigor and density, and compounding press disturbances, such as prolonged drought (Bentz and others 2010). Second, we inferred the behavior of autotrophic respiration from indirect measures that are made with high uncertainty (Bond-Lamberty and others 2004). Partitioning R_s into autotrophic and heterotrophic components remains notoriously challenging (Savage and others 2018). While the method we used to estimate R_h yields estimates comparable to those derived via independent approaches (Gough and others 2007), soil sieving eliminates physical structure and disrupts root-microbial interactions, creating artificial biological and physical conditions that limit the inference to field measurements. Third, we did not measure R_s continuously, omitting nighttime R_s as well as the peak dormant season. Finally, while our study captured 3-year responses, our analysis extends through only the initial resistance stage of disturbance response, and we anticipate substantial changes in R_s and its source components as canopy structure and microclimate shift, and mortality results in a large influx of detritus. Complete disturbance response cycles—from initial response through recovery—may occur over decades (Amiro and others 2010; Dorheim and others 2022), highlighting the need for long-term ecological observations.

Conclusions

The findings from our large-scale replicated manipulation of disturbance severity and type support several conclusions. First, our results of declining R_a with stable R_h in addition to findings showing stable NPP across the same disturbance continuum (Grigri and others 2020; Niedermaier and others 2022) suggests that net ecosystem production (NEP) was sustained—at least initially—even at high levels of phloem disruption. Placing our instantaneous R_s measurements in terms of cumulative R_s at our site (Curtis and others 2005), our observed 37% decline in R_s at the highest disturbance severity would translate to a loss of approximately 300 g C m^{-2} y^{-1}. This is comparable to total annual NEP at our site (Gough and others 2021b), suggesting the magnitude of R_s decline significantly changed ecosystem C balance. Second, our 3-year study, leveraging both absolute flux and relative resistance analyses, demonstrates that the effects of phloem disruption on R_s can be relatively long-lasting, underscoring the importance of multi-year observations. Third, we conclude that R_s responses to disturbance are conserved across different forest ecosystems on our upper Great Lakes landscape, suggesting a common physiological response to phloem disruption regardless of canopy composition. Finally, while this study assesses several years following a disturbance event, future work should prioritize synthesizing patterns and mechanisms of R_s recovery to the breadth of disturbance severities and types as well as disentangling variable outcomes of R_s disturbance response. Such synthetic, longer-term work will be critical for improving ecological forecasting of ecosystem C balance in an era of increasing and ever-changing disturbance regimes.

ACKNOWLEDGEMENTS

We thank the University of Michigan Biological Station for hosting our work and supporting our team members.

FUNDING

This work was funded by the National Science Foundation, Division of Environmental Biology (Award 1655095).

DATA AVAILABILITY

Data used in this analysis are available via the R FoRTE data package (*fortedata):* https://github.com/FoRTExperiment/fortedata. Statistical analysis, workflow and code used to visualize results are available via: https://github.com/kaylamathes/FoRTE_Rs.

Declarations

Conflict of interest The authors declare that they have no conflict of interest.

REFERENCES

Amiro BD. 2001. Paired-tower measurements of carbon and energy fluxes following disturbance in the boreal forest. Glob Chang Biol 7:253–268.

Amiro BD, Barr AG, Barr JG, Black TA, Bracho R, Brown M, Chen J, Clark KL, Davis KJ, Desai AR, and others. 2010. Ecosystem carbon dioxide fluxes after disturbance in forests of North America. J Geophys Res Biogeosci. https://doi.org/10.1029/2010JG001390.

Andersen CP, Nikolov I, Nikolova P, Matyssek R, Häberle KH. 2005. Estimating 'autotrophic' belowground respiration in

spruce and beech forests: Decreases following girdling. Eur J For Res 124:155–163.

Atkins JW, Bohrer G, Fahey RT, Hardiman BS, Morin TH, Stovall AEL, Zimmerman N, Gough CM. 2018. Quantifying vegetation and canopy structural complexity from terrestrial LiDAR data using the forestr r package. Methods Ecol Evol 9:2057–2066.

Atkins JW, Agee E, Barry A, Dahlin KM, Dorheim K, Grigri MS, Haber LT, Hickey LJ, Kamoske AG, Mathes K, and others. 2021. The fortedata R package: open-science datasets from a manipulative experiment testing forest resilience. Earth Syst Sci Data 13:943–952.

Atkins JW, Bond-Lamberty B, Fahey RT, Haber LT, Stuart-Haëntjens E, Hardiman BS, LaRue E, McNeil BE, Orwig DA, Stovall AEL, and others. 2020. Application of multidimensional structural characterization to detect and describe moderate forest disturbance. Ecosphere 11.

Ayres MP, Lombardero MJ. 2000. Assessing the consequences of global change for forest disturbance from herbivores and pathogens. Science of the Total Environment 262:263–286.

Bae K, Fahey TJ, Yanai RD, Fisk M. 2015. Soil Nitrogen Availability Affects Belowground Carbon Allocation and Soil Respiration in Northern Hardwood Forests of New Hampshire. Ecosystems 18:1179–1191.

Bai S, Qiu W, Zhang H, Wang Y, Berninger F. 2020. Soil respiration following Chinese fir plantation clear-cut: comparison of two forest regeneration approaches. Science of the Total Environment 709:135980.

Bentz BJ, Régnière J, Fettig CJ, Hansen EM, Hayes JL, Hicke JA, Kelsey RG, Negrón JF, Seybold SJ. 2010. Climate Change and Bark Beetles of the Western United States and Canada: Direct and Indirect Effects. Bioscience 60:602–613.

Bhupinderpal-Singh NA, Löfvenius MO, Högberg MN, Mellander PE, Högberg P. 2003. Tree root and soil heterotrophic respiration as revealed by girdling of boreal Scots pine forest: Extending observations beyond the first year. Plant Cell Environ 26:1287–96.

Binkley D, Stape JL, Takahashi EN, Ryan MG. 2006. Tree-girdling to separate root and heterotrophic respiration in two Eucalyptus stands in Brazil. Oecologia 148:447–454.

Bloemen J, Agneessens L, Van Meulebroek L, Aubrey DP, Mcguire MA, Teskey RO, Steppe K. 2014. Stem girdling affects the quantity of CO_2 transported in xylem as well as CO_2 efflux from soil. New Phytologist 201:897–907.

Bond-Lamberty B, Wang C, Gower ST. 2004. A global relationship between the heterotrophic and autotrophic components of soil respiration? Glob Chang Biol 10:1756–1766.

Bond-Lamberty B, Bailey VL, Chen M, Gough CM, Vargas R. 2018. Globally rising soil heterotrophic respiration over recent decades. Nature 560:80–83. https://doi.org/10.1038/s41586-018-0358-x.

Borkhuu B, Peckham SD, Ewers BE, Norton U, Pendall E. 2015. Does soil respiration decline following bark beetle induced forest mortality? Evidence from a lodgepole pine forest. Agric For Meteorol 214–215:201–207.

Buma B. 2015. Disturbance interactions: Characterization, prediction, and the potential for cascading effects. Ecosphere 6:1–15.

Busby PE, Canham CD. 2011. An exotic insect and pathogen disease complex reduces aboveground tree biomass in temperate forests of eastern North America. Canadian Journal of Forest Research 41:401–411.

Chen D, Zhang Y, Lin Y, Zhu W, Fu S. 2010. Changes in belowground carbon in *Acacia crassicarpa* and *Eucalyptus urophylla* plantations after tree girdling. Plant Soil 326:123–135.

Clippard EA, Haruna SI, Curtis PS, Clay C, Bond B, Mathes K, Vogel CS, Gough CM. 2022. Decadal forest soil respiration following stem girdling. Trees. https://doi.org/10.1007/s00468-022-02340-x.

Cohen WB, Yang Z, Stehman SV, Schroeder TA, Bell DM, Masek JG, Huang C, Meigs GW. 2016. Forest disturbance across the conterminous United States from 1985–2012: The emerging dominance of forest decline. For Ecol Manage 360:242–252.

Cooperdock SC, Hawkes CV, Xu DR, Breecker DO. 2020. Soil Water Content and Soil Respiration Rates Are Reduced for Years Following Wildfire in a Hot and Dry Climate. Global Biogeochem Cycles 34:1–18.

Curtis PS, Vogel CS, Gough CM, Schmid HP, Su HB, Bovard BD. 2005. Respiratory carbon losses and the carbon-use efficiency of a northern hardwood forest, 1999–2003. New Phytologist 167:437–456.

De Schepper V, Vanhaecke L, Steppe K. 2011. Localized stem chilling alters carbon processes in the adjacent stem and in source leaves. Tree Physiol 31:1194–1203.

Dietrich ST, MacKenzie MD. 2018. Comparing spatial heterogeneity of bioavailable nutrients and soil respiration in boreal sites recovering from natural and anthropogenic disturbance. Front Environ Sci 6:1–13.

Dorheim K, Gough CM, Haber LT, Mathes KC, Shiklomanov AN, Bond-Lamberty B. 2022. Climate Drives Modeled Forest Carbon Cycling Resistance and Resilience in the Upper Great Lakes Region, USA. J Geophys Res Biogeosci 127:1–15.

Duan S, He HS, Spetich MA, Wang WJ, Fraser JS, Xu W. 2022. Long-term effects of succession, climate change and insect disturbance on oak-pine forest composition in the U.S. Central Hardwood Region. Eur J For Res 141:153–164.

Edgar CB, Westfall JA. 2022. Timing and extent of forest disturbance in the Laurentian Mixed Forest. Frontiers in Forests and Global Change 5:1–15.

Ekberg A, Buchmann N, Gleixner G. 2007. Rhizospheric influence on soil respiration and decomposition in a temperate Norway spruce stand. Soil Biol Biochem 39:2103–2110.

Flower CE, Knight KS, Gonzalez-Meler MA. 2013. Impacts of the emerald ash borer (*Agrilus planipennis* Fairmaire) induced ash (*Fraxinus* spp.) mortality on forest carbon cycling and successional dynamics in the eastern United States. Biol Invasions 15:931–944.

Frey B, Hagedorn F, Giudici F. 2006. Effect of girdling on soil respiration and root composition in a sweet chestnut forest. For Ecol Manage 225:271–277.

Gaumont-Guay D, Black A, Barr AG, Jassal RS, Nesic Z. 2008. Biophysical controls on rhizospheric and heterotrophic components of soil respiration in a boreal black spruce stand. Tree Physiology 28:161–171.

Gough CM, Vogel CS, Harrold KH, George K, Curtis PS. 2007. The legacy of harvest and fire on ecosystem carbon storage in a north temperate forest. Glob Chang Biol 13:1935–1949.

Gough CM, Vogel CS, Schmid HP, Su HB, Curtis PS. 2008. Multi-year convergence of biometric and meteorological estimates of forest carbon storage. Agric For Meteorol 148:158–170.

Gough CM, Curtis PS, Hardiman BS, Scheuermann CM, Bond-Lamberty B. 2016. Disturbance, complexity, and succession of net ecosystem production in North America's temperate deciduous forests. Ecosphere 7:1–15.

Gough CM, Atkins JW, Bond-Lamberty B, Agee EA, Dorheim KR, Fahey RT, Grigri MS, Haber LT, Mathes KC, Pennington SC, Shiklomanov AN, Tallant JM. 2021a. Forest Structural Complexity and Biomass Predict First-Year Carbon Cycling Responses to Disturbance. Ecosystems 24:699–712.

Gough CM, Bohrer G, Hardiman BS, Nave LE, Vogel CS, Atkins JW, Bond-Lamberty B, Fahey RT, Fotis AT, Grigri MS, and others. 2021b. Disturbance-accelerated succession increases the production of a temperate forest. Ecological Applications 31:1–17.

Gough CM, Atkins JW, Fahey RT, Curtis PS, Bohrer G, Hardiman BS, Hickey LJ, Nave LE, Niedermaier KM, Clay C, Tallant JM, Bond-Lamberty B. 2022. Disturbance has variable effects on the structural complexity of a temperate forest landscape. Ecol Indic 140.

Grigri MS, Atkins JW, Vogel C, Bond-Lamberty B, Gough CM. 2020. Aboveground wood production is sustained in the first growing season after phloem-disrupting disturbance. Forests 11:1–19.

Harmon ME, Bond-Lamberty B, Tang J, Vargas R. 2011. Heterotrophic respiration in disturbed forests: A review with examples from North America. J Geophys Res Biogeosci 116:1–17.

Hicke JA, Allen CD, Desai AR, Dietze MC, Hall RJ, Hogg EHT, Kashian DM, Moore D, Raffa KF, Sturrock RN, Vogelmann J. 2012. Effects of biotic disturbances on forest carbon cycling in the United States and Canada. Glob Chang Biol 18:7–34.

Hillebrand H, Langenheder S, Lebret K, Lindström E, Östman Ö, Striebel M. 2018. Decomposing multiple dimensions of stability in global change experiments. Ecol Lett 21:21–30.

Högberg MN, Högberg P. 2002. Extramatrical ectomycorrhizal mycelium contributes one-third of microbial biomass and produces, together with associated roots, half the dissolved organic carbon in a forest soil. New Phytologist 154:791–795.

Högberg P, Nyberg G, Taylor AFS, Ekblad A, Ho MN, Read DJ, Ottosson-lo M. 2001. Large-scale forest girdling shows that current photosynthesis drives soil respiration. Nature 411:789–792.

Hu T, Sun L, Hu H, Guo F. 2017. Effects of fire disturbance on soil respiration in the non-growing season in a Larix gmelinii forest in the Daxing'an Mountains, China. PLoS One. https://doi.org/10.1371/journal.pone.0180214.

Ivanov AV, Salo MA, Tolstikova VY, Bryanin SV, Zamolodchikov DG. 2022. Effects of Windfall on Soil Surface Carbon Emission and Fine Root Stocks in the Central Sikhote-Alin. Eurasian Soil Science 55:1405–1413.

Kang H, Fahey TJ, Bae K, Fisk M, Sherman RE, Yanai RD, See CR. 2016. Response of forest soil respiration to nutrient addition depends on site fertility. Biogeochemistry 127:113–124.

Kelly J, Ibáñez TS, Santín C, Doerr SH, Nilsson MC, Holst T, Lindroth A, Kljun N. 2021. Boreal forest soil carbon fluxes one year after a wildfire: Effects of burn severity and management. Glob Chang Biol 27:4181–4195.

Ledo A, Paul KI, Burslem DFRP, Ewel JJ, Barton C, Battaglia M, Brooksbank K, Carter J, Eid TH, England JR, and others. 2018. Tree size and climatic water deficit control root to shoot ratio in individual trees globally. New Phytologist 217:8–11.

Lei J, Guo X, Zeng Y, Zhou J, Gao Q, Yang Y. 2021. Temporal changes in global soil respiration since 1987. Nat Commun 12:1–9. https://doi.org/10.1038/s41467-020-20616-z.

Lenth R (2022) emmeans: Estimated Marginal Means, aka Least-Squares Means

Levy-Varon JH, Schuster WSF, Griffin KL. 2012. The autotrophic contribution to soil respiration in a northern temperate deciduous forest and its response to stand disturbance. Oecologia 169:211–220.

Levy-Varon JH, Schuster WSF, Griffin KL. 2014. Rapid rebound of soil respiration following partial stand disturbance by tree girdling in a temperate deciduous forest. Oecologia 174:1415–1424.

Masyagina OV, Hirano T, Ji DH, Choi DS, Qu L, Fujinuma Y, Sasa K, Matsuura Y, Prokushkin SG, Koike T. 2006. Effect of spatial variation of soil respiration rates following disturbance by timber harvesting in a larch plantation in northern Japan. Forest Sci Technol 2:80–91.

Mathes KC, Ju Y, Kleinke C, Oldfield C, Bohrer G, Bond-Lamberty B, Vogel CS, Dorheim K, Gough CM. 2021. A multidimensional stability framework enhances interpretation and comparison of carbon cycling response to disturbance. Ecosphere 12:e03800.

Mayer M, Matthews B, Rosinger C, Sandén H, Godbold DL, Katzensteiner K. 2017. Tree regeneration retards decomposition in a temperate mountain soil after forest gap disturbance. Soil Biol Biochem 115:490–498.

de Mendiburu F. 2021. _agricolae: Statistical Procedures for Agricultural Research_. R package.

Meyer N, Welp G, Amelung W. 2018. The Temperature Sensitivity (Q10) of Soil Respiration: Controlling Factors and Spatial Prediction at Regional Scale Based on Environmental Soil Classes. Global Biogeochem Cycles 32:306–323.

Moore DJP, Trahan NA, Wilkes P, Quaife T, Stephens BB, Elder K, Desai AR, Negron J, Monson RK. 2013. Persistent reduced ecosystem respiration after insect disturbance in high elevation forests. Ecol Lett 16:731–737.

Nave LE, Gough CM, Maurer KD, Bohrer G, Hardiman BS, Le Moine J, Munoz AB, Nadelhoffer KJ, Sparks JP, Strahm BD, and others. 2011. Disturbance and the resilience of coupled carbon and nitrogen cycling in a north temperate forest. J Geophys Res Biogeosci 116:1–14.

Nave LE, Walters BF, Hofmeister KL, Perry CH, Mishra U, Domke GM, Swanston CW. 2019. The role of reforestation in carbon sequestration. New For (Dordr) 50:115–137.

Niedermaier KM, Atkins JW, Grigri MS, Bond-lamberty B, Gough CM. 2022. Structural complexity and primary production resistance are coupled in a temperate forest. Frontiers in Forests and Global Change. https://doi.org/10.3389/ffgc.2022.941851.

Pearsall DR, Barnes B V, Zogg GR, Lapin M, Ring RR, Ring D. 1995. Landscape ecosystems of the University of Michigan Biological Station. School of Natural Resources & Environment. 66.

R Core Team. 2022. R: A language and environment for statistical computing.

Sampson DA, Janssens IA, Curiel Yuste J, Ceulemans R. 2007. Basal rates of soil respiration are correlated with photosynthesis in a mixed temperate forest. Glob Chang Biol 13:2008–2017.

Savage KE, Davidson EA, Abramoff RZ, Finzi AC, Giasson MA. 2018. Partitioning soil respiration: quantifying the artifacts of the trenching method. Biogeochemistry 140:53–63.

Scott-Denton LE, Rosenstiel TN, Monson RK. 2006. Differential controls by climate and substrate over the heterotrophic and

rhizospheric components of soil respiration. Glob Chang Biol 12:205–216.

Seidl R, Thom D, Kautz M, Martin-Benito D, Peltoniemi M, Vacchiano G, Wild J, Ascoli D, Petr M, Honkaniemi J, and others. 2017. Forest disturbances under climate change. Nat Clim Chang 7:395–402. https://doi.org/10.1038/nclimate3303.

Sommerfeld A, Senf C, Buma B, D'Amato AW, Després T, Díaz-Hormazábal I, Fraver S, Frelich LE, Gutiérrez ÁG, Hart SJ, and others. 2018. Patterns and drivers of recent disturbances across the temperate forest biome. Nat Commun 9:4355. https://doi.org/10.1038/s41467-018-06788-9.

Stuart-Haëntjens EJ, Curtis PS, Fahey RT, Vogel CS, Gough CM. 2015. Net primary production of a temperate deciduous forest exhibits a threshold response to increasing disturbance severity. Ecology 96:2478–2487.

Subke JA, Voke NR, Leronni V, Garnett MH, Ineson P. 2011. Dynamics and pathways of autotrophic and heterotrophic soil CO2 efflux revealed by forest girdling. Journal of Ecology 99:186–193.

Sun L, Hu T, Kim JH, Guo F, Song H, Lv X, Hu H. 2014. The effect of fire disturbance on short-term soil respiration in typical forest of Greater Xing'an Range, China. J For Res (Harbin) 25:613–620.

Wickham H. 2016. ggplot2: Elegant Graphics for Data Analysis.

Wilson DC, Morin RS, Frelich LE, Ek AR. 2019. Monitoring disturbance intervals in forests: a case study of increasing forest disturbance in Minnesota. Ann For Sci 76.

Xu S, Eisenhauer N, Pellegrini AFA, Wang J, Certini G, Guerra CA, Lai DYF. 2022. Fire frequency and type regulate the response of soil carbon cycling and storage to fire across soil depths and ecosystems: A meta-analysis. Science of the Total Environment 825:153921.

Yan Y, Quan Q, Meng C, Wang J, Tian D, Wang B, Zhang R, Niu S. 2021. Varying soil respiration under long-term warming and clipping due to shifting carbon allocation toward belowground. Agric for Meteorol 304–305:108408.

Yuan ZY, Chen HYH. 2013. Effects of Disturbance on Fine Root Dynamics in the Boreal Forests of Northern Ontario, Canada. Ecosystems 16:467–477.

Zhao S, Chen K, Wu C, Mao Y. 2018. Effects of simulated warming on soil respiration to XiaoPo lake. IOP Conf Ser Earth Environ Sci 113.